Response of meteoric $\delta^{18}O$ to surface uplift — Implications for Cenozoic Andean Plateau growth

Nadja Insel [a,*,1], Christopher J. Poulsen [a,1], Todd A. Ehlers [b], Christophe Sturm [c]

[a] Department of Geological Sciences, University of Michigan, Ann Arbor, MI 48109-1005, USA
[b] Institut für Geowissenschaften, Universität Tübingen, D-72074, Tübingen, Germany
[c] Department of Geology and Geochemistry, Stockholm University, 106 91 Stockholm, Sweden

ARTICLE INFO

ABSTRACT

The timing and magnitude of surface uplift provide important constraints on geodynamic models of orogen formation. Oxygen isotope ($\delta^{18}O$) and mass-47 isotopolog (Δ_{47}) compositions from terrestrial carbonate sediments have been used with modern isotope and temperature lapse rates to infer past surface elevations of the Andes. However, these paleoaltimetry interpretations are contentious because variations in the oxygen isotope composition of meteoric water ($\delta^{18}O_p$) are caused by changes in elevation (orographic) and regional climate. Here, we use a limited-domain isotope-tracking general circulation model to simulate changes in $\delta^{18}O_p$ and isotopic lapse rates in response to Andean surface uplift, and to re-evaluate $\delta^{18}O$ and Δ_{47} changes in late Miocene carbonates previously associated with rapid Andean growth. Results indicate that Andean surface uplift leads to changes in low-level atmospheric circulation and an increase in precipitation along the eastern Andean flank which influences isotopic source and amount effects. Simulated changes in Andean $\delta^{18}O_p$ are not systematic with an increase in surface elevation, but are instead a function of orographic thresholds that abruptly change regional climate. A $\delta^{18}O_p$ decrease of $>5‰$ over the central Andes and an increase in isotopic lapse rates (up to $0.8‰\,km^{-1}$) coincide with Andean surface uplift from 75 to 100% of modern elevation. These changes in the isotopic signature could account for the entire 3–4‰ $\delta^{18}O$ depletion in late Miocene carbonate nodules, and suggest an Andean paleoelevation of ~3000 m (75% of modern elevations) before 10 Ma.

© 2011 Elsevier B.V. All rights reserved.

1. Introduction

The timing and rates at which current Andean Plateau (AP) elevations were attained are debated. A rapid and recent rise of ~2.5 ± 1 km between 10 and 6 Ma has been proposed based on $\delta^{18}O$ and mass-47 isotopolog (Δ_{47}) compositions ('clumped isotopes') of late Miocene terrestrial carbonates (e.g. Garzione et al., 2006, 2008; Ghosh et al., 2006b). This interpretation has been questioned by paleoclimate modeling studies that have highlighted the sensitivity of stable isotope paleoaltimetry interpretations to climate change (Ehlers and Poulsen, 2009; Insel et al. 2009; Poulsen et al., 2010). Furthermore, geological and recent biotaxa evidence suggests AP growth was slow and steady since at least the Eocene (~40 Ma), and implies elevations of ~2000 m prior to 20–10 Ma (e.g. Alpers and Brimhall, 1988; Barnes and Ehlers, 2009; Picard et al., 2008; Rech et al., 2006; Schlunegger et al., 2010; Sebrier et al., 1988). Thus, significant debate exists on the elevation history of the AP and the influence of climate change on paleoelevation reconstructions.

Oxygen isotope paleoaltimetry uses $\delta^{18}O$ preserved in geological archives (e.g. carbonates, silicates, volcanic glasses) as a proxy for ancient meteoric $\delta^{18}O$. The composition of $\delta^{18}O$ ($\delta^{18}O = ([(^{18}O/^{16}O)_{sample}/(^{18}O/^{16}O)_{standard}] - 1) * 1000$) in these archives is controlled by the temperature and the composition of meteoric water at the time of mineral formation, both of which are related to elevation (e.g. Chamberlain et al., 1999; Drummond et al., 1993; Siegenthaler and Oeschger, 1980). The elevation–$\delta^{18}O$ relationship reflects Rayleigh distillation of the heavy isotope (^{18}O) through condensation and precipitation as air masses are adiabatically cooled. Due to the correlation between $\delta^{18}O$ of meteoric water ($\delta^{18}O_p$) and elevation, mountain surface uplift can be reconstructed through stable isotope studies of authigenic (in-situ formed) minerals, assuming that past isotopic lapse rates ($\Gamma_{\delta^{18}O}$, the rate of changes in isotopic ratio with altitude) were analogous to modern rates. Based on these assumptions, a 3–4‰ $\delta^{18}O$ shift in late Miocene carbonate nodules from the AP has been interpreted to reflect ~2.5 km of surface uplift (Garzione et al., 2006; Ghosh et al., 2006b).

However, factors other than elevation change influence the modern climatology of $\delta^{18}O_p$ along the Andes, such as precipitation (amount effect), water vapor source, wind patterns, ENSO, and remote climate pattern (e.g. Sepulchre et al., 2009; Sturm et al., 2007b; Vuille et al., 2003). General atmospheric circulation models indicate that Andean surface uplift causes substantial changes in

* Corresponding author. Tel.: + 1 734 647 5636.
E-mail address: nadinsel@uchicago.edu (N. Insel).
[1] Present address at the Department of the Geophysical Sciences, University of Chicago, Chicago, IL 60637.

South American regional climate (e.g. Ehlers and Poulsen, 2009; Garreaud et al., 2010; Insel et al., 2009; Poulsen et al., 2010). In particular, an abrupt increase in Andean precipitation and convection is associated with Andean threshold elevations of 50–70% of modern heights (Insel et al., 2009; Poulsen et al., 2010). These changes in regional paleoclimate can influence isotopic fractionation and source effects that cause dramatic changes in the paleo-$\delta^{18}O$ composition (Ehlers and Poulsen, 2009). Thus, late Miocene changes in central Andean $\delta^{18}O$ could be related to the intensification of precipitation associated with relatively minor surface uplift (Poulsen et al., 2010).

The clumped isotope carbonate thermometer has been used as an independent approach to paleoelevation reconstructions. This technique relies on the temperature dependence of the abundance of bonds between rare, heavy isotopes (i.e. $^{13}C^{18}O^{16}O$) in the carbonate mineral lattice, expressed as Δ_{47} (the ratio of mass 47 to mass 44 isotopologs in a sample from that ratio expected for a stochastic distribution of isotopes in that sample) (Ghosh et al., 2006a; Ghosh et al., 2006b). The ordering, or 'clumping', of heavy isotopes into bonds with each other is favored at low temperatures and the growth temperature of a carbonate mineral can be defined by the analysis of the isotopic constituents of the carbonate alone. The Δ_{47} derived temperatures have been used to reconstruct Andean paleoelevations assuming modern temperature lapse rates with elevation (Ghosh et al., 2006b). However, it has been shown that an increase in Andean plateau elevations not only results in adiabatic cooling directly linked to elevation gain, but also in non-adiabatic cooling associated with regional climate change (Ehlers and Poulsen, 2009). That could lead to a change in temperature lapse rates over time and influence paleoaltimetry estimations based on temperature changes.

Previous studies have implemented either high-resolution non-isotope tracking regional models (e.g. Ehlers and Poulsen, 2009; Insel et al., 2009) or global climate models with isotope tracking capabilities (e.g. Jeffery et al., 2011; Poulsen et al., 2010). In this study we extend this previous work by using a high-resolution limited-domain general circulation model with isotope diagnostics (REMOiso). In comparison to global spectral climate models, the limited-domain model provides a better representation of Andean topography at a horizontal resolution that approaches the spatial scales represented by proxy data. Results highlight the behavior of $\delta^{18}O_p$ and temperature under past topographic and climate conditions and refine orographic threshold elevations for significant changes in $\delta^{18}O_p$. Specifically, we (1) estimate changes in $\delta^{18}O_p$ due to Andean surface uplift and provide predictions of precipitation patterns and $\delta^{18}O_p$ for specific Andean heights; (2) quantify the changes in isotopic lapse rates in response to Andean surface uplift; and (3) evaluate the geological/isotopic evidence for surface uplift with specific focus on Δ_{47} estimates. The integration of model results and observations suggests that regional climate change in response to surface uplift caused changes in the stable isotope record.

2. Method

To quantify the influence of Andean surface uplift on $\delta^{18}O_p$ and oxygen isotopic lapse rates, we use a numerical three-dimensional limited-domain general circulation model with isotope-tracking capabilities (REMOiso) (Sturm et al., 2005; Sturm et al., 2007a). Isotope fractionation and transport processes are embedded at all stages of the hydrological cycle by defining isotopic counterparts to all water-related variables. Therefore, the species H_2O^{18} and HDO are treated independently from the predominant H_2O^{16}, but undergo the same processes including equilibrium and kinetic fractionations (Sturm et al., 2005). Stable water isotopologs are treated as passive tracers in soil moisture and snow layer and all vapor fluxes from the surface are considered non-fractionating. All experiments are forced using modern boundary conditions, including stable water isotopes, from

the ECHAM-4 global climate model with specified SSTs derived from monthly satellite data (i.e. HadSST; Hoffmann et al., 1998).

Simulations were performed for South America using a continental-scale domain with a horizontal grid spacing of 0.5° (~55 km) and 31 vertical levels. Three experiments were completed with Andean elevations representing 100%, 75%, and 50% of the modern Andes height. In other regions of South America, the topography was maintained at modern elevations. All other parameters remain the same between experiments. All three experiments were integrated over the ten-year period from 1989 to 1998. Because of the high computational cost, it was not practical to run REMOiso continuously over this time span. Instead, 15-month integrations, starting from the previous year's October and running through December of the simulation year, were completed. Each simulation year was initialized from the same initial conditions from a 21-month (January to September) simulation forced with boundary conditions for year 1993. Year 1993 was chosen for the spin-up, because it most closely resembled the 30-yr precipitation mean over the study area.

We present simulated annual amount-weighted mean $\delta^{18}O_p$ and isotopic lapse rates based on 10-year averages. Isotopic lapse rates are calculated every 0.5° latitude by linear regression of $\delta^{18}O_p$ for all grid points between peak and flank (~300 m) elevations. Absolute values of isotopic lapse rates are presented as a 4-point (~2° latitudinal) running zonal average. We note that by definition the lapse rate is defined as the rate of decrease of an atmospheric variable (e.g. temperature) with height. However, to be consistent with previous studies, we report isotopic lapse rates as the change in $\delta^{18}O_p$ with altitude. Thus, a $\delta^{18}O_p$ decrease of $-1\permil\,km^{-1}$ elevation gain is reported as a lapse rate of $-1\permil\,km^{-1}$, rather than $1\permil\,km^{-1}$. However, as changes in isotopic lapse rates are described as changes in absolute magnitude, an increase in lapse rate is consistent with a more negative lapse rate (i.e. an increase from $-1.5\permil\,km^{-1}$ to $-2\permil\,km^{-1}$).

3. Results

3.1. Modern isotope climatology

REMOiso has been shown to realistically simulate modern large-scale climate and circulation patterns, and spatial variations in $\delta^{18}O_p$ in South America (Sturm et al., 2007a; Sturm et al., 2007b). In agreement with observations, simulated $\delta^{18}O_p$ is relatively high (-3 to $-6\permil$) over the Amazon Basin due to evapotranspiration (Fig. 1b, 100% Andes). Once air masses reach the Andes, adiabatic cooling and condensation associated with rising air masses contribute to the isotopic depletion of vapor. Strong convergence, vertical ascent and rainout along the eastern Andean flank result in Rayleigh distillation which causes $\delta^{18}O_p$ to exponentially decrease with cumulative precipitation, and results in the lowest $\delta^{18}O_p$ ($<-12\permil$) at high elevation sites along the Andes (Fig. 1b). Low $\delta^{18}O_p$ (-7 to $-10\permil$) is also simulated in southern South America due to the latitudinal effect.

Simulated modern isotopic lapse rates ($\Gamma_{\delta18O}$) vary significantly along the Andes (Fig. 2a and e). Along the eastern flank, modern average $\Gamma_{\delta18O}$ range from $-2.09\permil\,km^{-1}$ to $1.02\permil\,km^{-1}$ between 10°N and 50°S (Fig. 2a). Along the western flank, simulated modern average $\Gamma_{\delta18O}$ vary between $-3.46\permil$ and $0.22\permil\,km^{-1}$ (Fig. 2e). Overall, the largest (most negative) lapse rates exist over the AP at ~20°S and in the southern Andes south of ~37°S. Lapse rates can be positive ($\delta^{18}O_p$ increases with altitude) where modern peak elevations in the model are below 2000 m (Fig. 2a, b, e). In the southern Andes, positive $\Gamma_{\delta18O}$ along the eastern flank are mainly related to an isotopic rain shadow effect, where the steady eastward decrease in $\delta^{18}O_p$ reflects the increasing distance from the principle water vapor source (South Pacific) (Stern and Blisniuk, 2002) and spillover of condensate to the leeward (eastern) side leads to further depletion
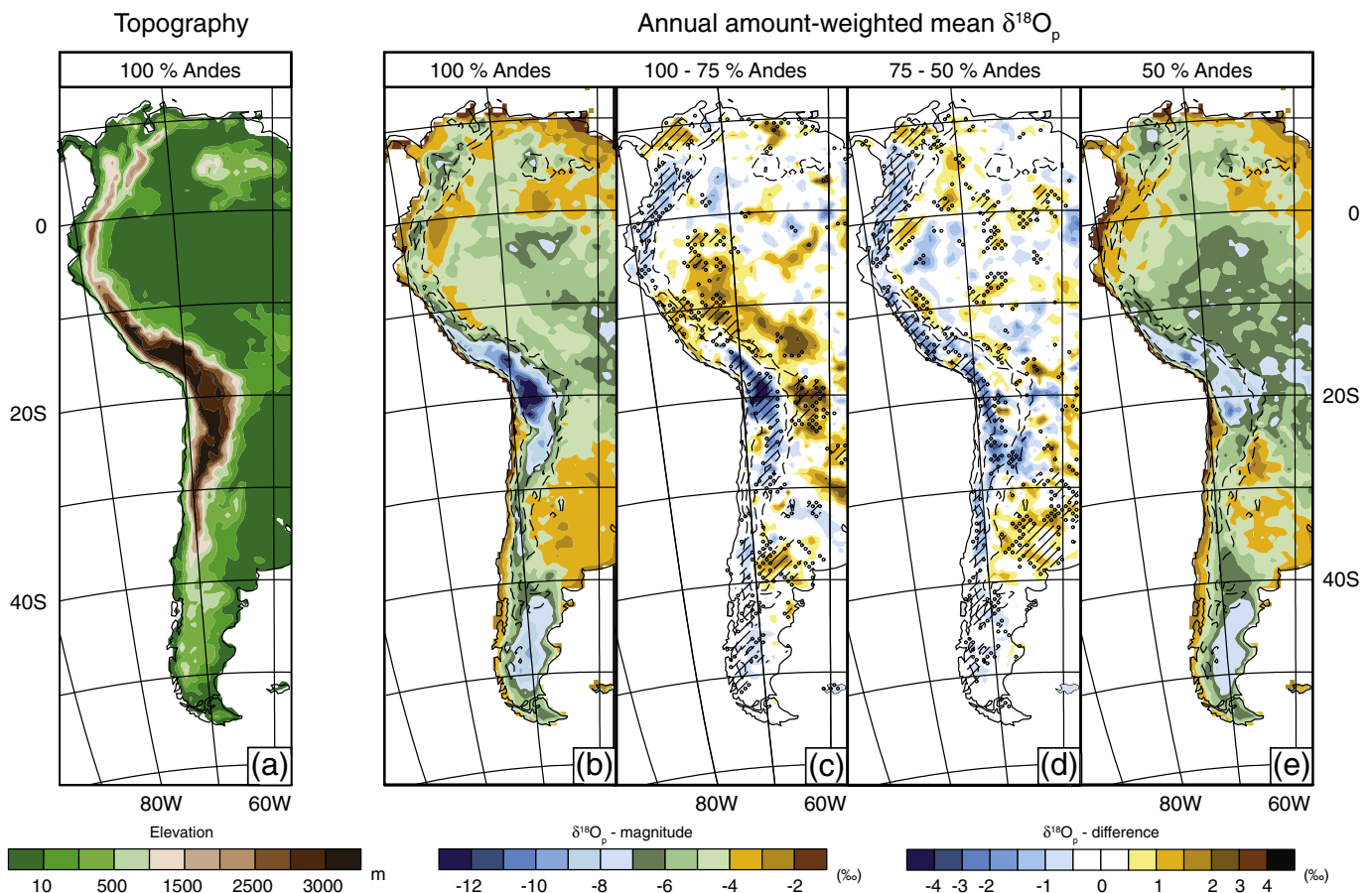
Fig. 1. Topography and annual amount-weighted mean $\delta^{18}O_p$ (‰) along the Andes. Dashed lines represent 1000 and 3000 m contour lines. (a) Present-day topography (m) used in the model for 100% Andes simulations. (b–e) Panel plots showing changes in $\delta^{18}O_p$ with increasing Andean elevations. (e) Absolute values of $\delta^{18}O_p$ for 50% Andean height simulations, (d) difference in $\delta^{18}O_p$ between 75 and 50% Andes, (c) difference in $\delta^{18}O_p$ between 100 and 75% Andes, and (b) absolute $\delta^{18}O_p$ compositions for simulations with 100% Andes, respectively. Stippled circle regions show areas where $\delta^{18}O_p$ changes are significant at the 80–90% confidence level, dashed pattern indicates regions where $\delta^{18}O_p$ changes are significant at the >90% confidence level.

of $\delta^{18}O_p$ in air masses along the eastern flank with decreasing altitude.

The simulated mean annual $\Gamma_{\delta18O}$ across the eastern flank of the northern Andean Plateau (~14.5–19°S) is -1.27 ± 0.31‰ km^{-1} with isotopic lapse rates for individual years ranging between -0.66 and -1.67‰ km^{-1}. Simulated mean summer (DJF) $\Gamma_{\delta18O}$ is -1.58 ± 0.36‰ km^{-1} with $\Gamma_{\delta18O}$ for individual years varying between -1.08 and -2.37‰ km^{-1}. In comparison, meteorological stations across that transect report annual $\Gamma_{\delta18O}$ from -1.46‰ km^{-1} in a dry year to -2.39‰ km^{-1} in a wet year with a mean annual $\Gamma_{\delta18O}$ of -2.12‰ km^{-1} (Gonfiantini et al., 2001). The observed absolute $\delta^{18}O$ values for individual stations are in very good agreement with model results (Suppl. 1). The calculated isotopic lapse rates based on observations are slightly larger than simulated lapse rate, most likely due to differences in the spatial and temporal scales of both datasets. For example, observations are biased to higher elevations and, therefore, more negative $\delta^{18}O$ values due to a lack of sample coverage at intermediate elevations between 1500 and 4000 m, which could result in an overestimation of $\Gamma_{\delta18O}$ (Suppl. 1). In contrast, model simulations are limited in the absolute height of the Andes, which could result in an underestimation of Rayleigh fractionation along the flank and smaller $\Gamma_{\delta18O}$ at high elevations. However, the overall observed variability in $\Gamma_{\delta18O}$ (e.g. temporal variability in $\Gamma_{\delta18O}$ by ~1‰ km^{-1} between individual years) is very well captured in the model.

In the context of interannual variability, we note that there is a fundamental mismatch between paleodata and observational data. As a result of the slow precipitation of carbonates, paleodata generally represent time-averages of thousands of years. Observational data

typically span only a few years and often have missing monthly $\delta^{18}O$ values (generally from the drier, higher $\delta^{18}O$ months), which bias the record towards anomalous wet events (e.g. ENSO). Thus, paleoaltimetry essentially uses modern 'snapshots' to interpret past records that represent much longer time periods. In fact, Andean Plateau paleoaltimetry estimates have been based on an isotopic lapse rate that has been calculated based on one year of precipitation-unweighted mean $\delta^{18}O$ records across an individual transect in the central Andes (Garzione et al., 2006; Garzione et al., 2008). Thus, while it is reassuring that our climate model capture observed interannual $\delta^{18}O_p$ variability, our view is that $\delta^{18}O$ lapse rates and $\delta^{18}O$ variability in the Andes are not well constrained and introduce an important source of uncertainty to paleoaltimetry estimates.

3.2. Sensitivity of $\delta^{18}O_p$ to surface uplift

In comparison to the modern, $\delta^{18}O_p$ in lower elevation simulations is larger (up to >7‰) over regions of high elevation, but smaller by approximately 2–3‰ in the lowlands (compare Fig. 1b–e). A decrease in Andean $\delta^{18}O_p$ with increasing elevation is expected from the altitude effect. However, the decrease in $\delta^{18}O_p$ over the central Andes (5–30°S) is not systematic with an increase in surface elevation, but differs in magnitude and timing across the Andean Plateau (AP). For example, the southern AP (24–28°S) experiences the largest decline in $\delta^{18}O_p$ (3–4‰) between the 50 and 75% elevation scenarios, while the northern/central AP region (14–24°S) experiences the largest $\delta^{18}O_p$ decrease (>5‰) between the 75 and 100% cases (Fig. 1b–e). To understand the isotopic response to surface uplift on regional
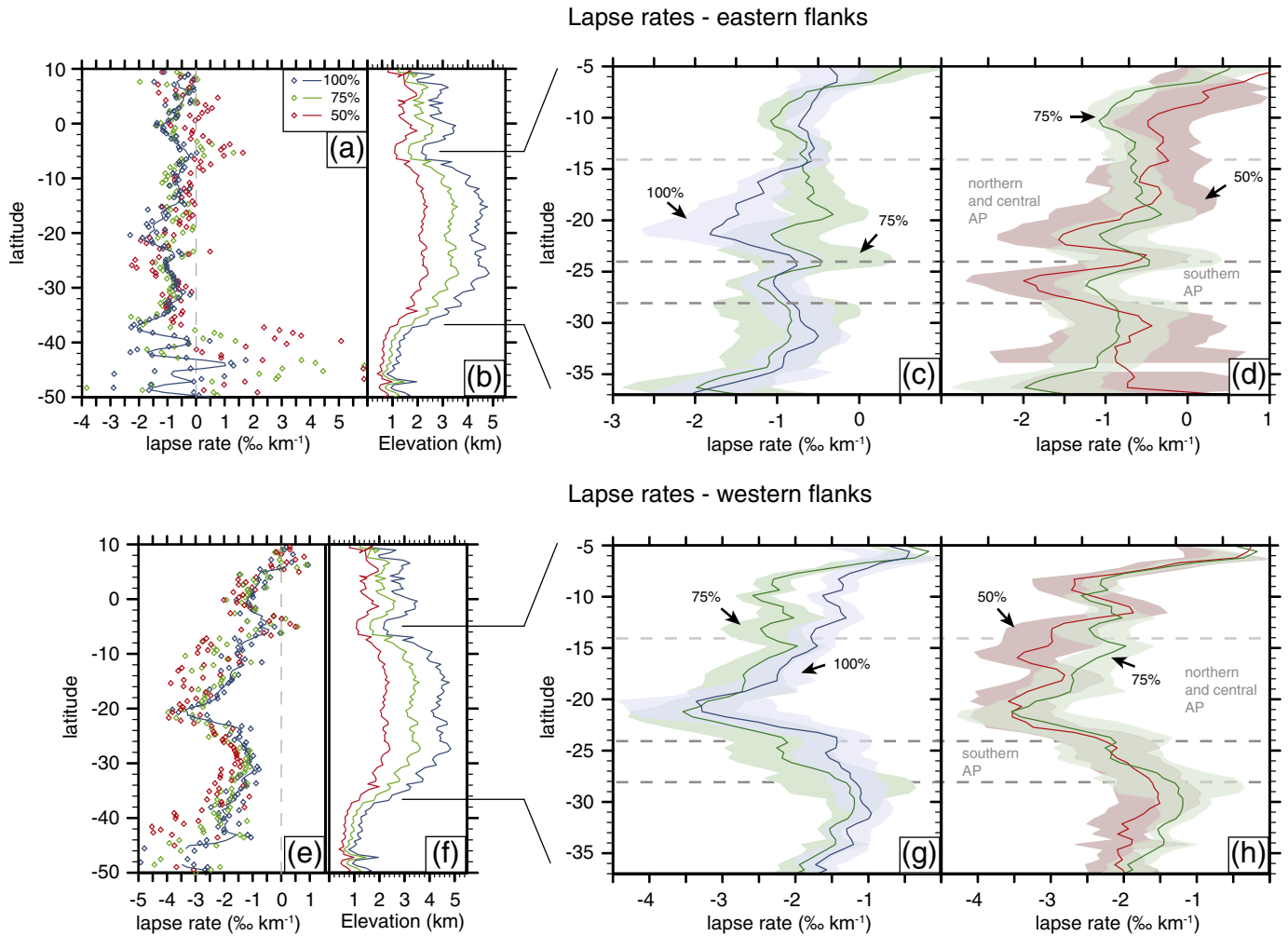
Fig. 2. Isotopic lapse rates along the eastern (a–d) and western (e–g) flank of the Andes for different height scenarios (100%, 75%, and 50% of the modern elevation). (a) All calculated lapse rates (‰ km^{-1}) between 10°N and 50°S. Diamonds represent simulated lapse rates for each latitudinal transect; colored lines represent the 2 degree running average through the data. The gray dashed line highlights the zero line. (b) Maximum elevation along the Andes for different simulation scenarios. (c–d) Isotopic lapse rates (‰ km^{-1}) between 5° and 35°S. Solid lines represent mean isotopic lapse rates, and the shaded area is the 1σ standard deviation calculated from the 10 year simulation. Gray dashed lines represent borders of the northern and central Andean Plateau (AP), and the southern part of the AP, respectively. Despite large variations in annual isotopic lapse rates, we suggest that because the changes in mean isotopic lapse rates reflect large-scale climatological changes associated with surface uplift they are instructive of past lapse rate changes. (e, f, g, h) Same as a, b, c, and d, but for the western flank of the Andes.

scales, in the following we discuss the progressive $\delta^{18}O_p$ changes associated with Andean uplift from 50 to 100% of their modern heights. Our analysis is focused on regions where the changes in the isotopic concentration are significant at the 80% confidence level (based on Student's t test; Fig. 1).

Uplift of the Andes from 50 to 75% of modern surface elevations leads to a $\delta^{18}O_p$ decrease of ~2–4‰ over the high elevation Andes (Fig. 1d), while the $\delta^{18}O_p$ along the eastern flank increases slightly. The overall decrease in $\delta^{18}O_p$ over the high Andes is related to the initiation/strengthening of the South American low-level jet (SALLJ). A strong SALLJ intensifies convergence, orographic lifting, and latent heat release, which fuels convection and convective condensation (Insel et al., 2009). Greater precipitation rate along the eastern Andean flank (Fig. 3d) results in stronger isotopic fractionation through Rayleigh distillation over the high Andes. Along the eastern flank of the southern AP region, the establishment of the SALLJ intensifies transport of isotopically depleted moisture from the north that leads to a decrease in $\delta^{18}O_p$ along the eastern flank (Fig. 1d). The isotopically depleted vapor replaces relatively enriched vapor sourced from the South Atlantic region. However, south of 30°S, where the SALLJ terminates, $\delta^{18}O_p$ increases in the Andean foreland due to a southward

shift and intensification of the subtropical high. The changes in position and magnitude of the subtropical high cause an enhanced influx of $\delta^{18}O_p$ enriched air masses from the subtropical region and lower influx from the isotopically more depleted mid-latitude regions.

Uplift of the Andes from 75 to 100% of modern elevation causes a substantial (up to 6‰) decrease in $\delta^{18}O_p$ over the AP (Fig. 1c), and an increase in $\delta^{18}O_p$ by ~3‰ along the eastern flank. These changes are related to weaker convergence over the Amazon Basin and the amplification of the SALLJ (Insel et al., 2009). A reduction in moisture convergence over the Amazon Basin, associated with a strengthening in the low-pressure system over the central Andes that draws in the moisture from the Amazon Basin, leads to a decrease in precipitation (Fig. 3c) and an increase in $\delta^{18}O_p$ over the (south-)western part of the Amazon Basin (Fig. 1c). Northeasterly winds transport this enriched vapor from the Amazon Basin to the Andean lowlands and increase $\delta^{18}O_p$ compositions along the eastern Andean flank. Moreover, the stronger SALLJ causes enhanced convergence and rainout (Insel et al., 2009) that leads to stronger isotopic fractionation through Rayleigh distillation over the high Andes. Interestingly, $\delta^{18}O_p$ increases by 1–2‰ over the high Andes between 7 and 14°S. In this region, isotopic enrichment at high elevations is consistent

Topography

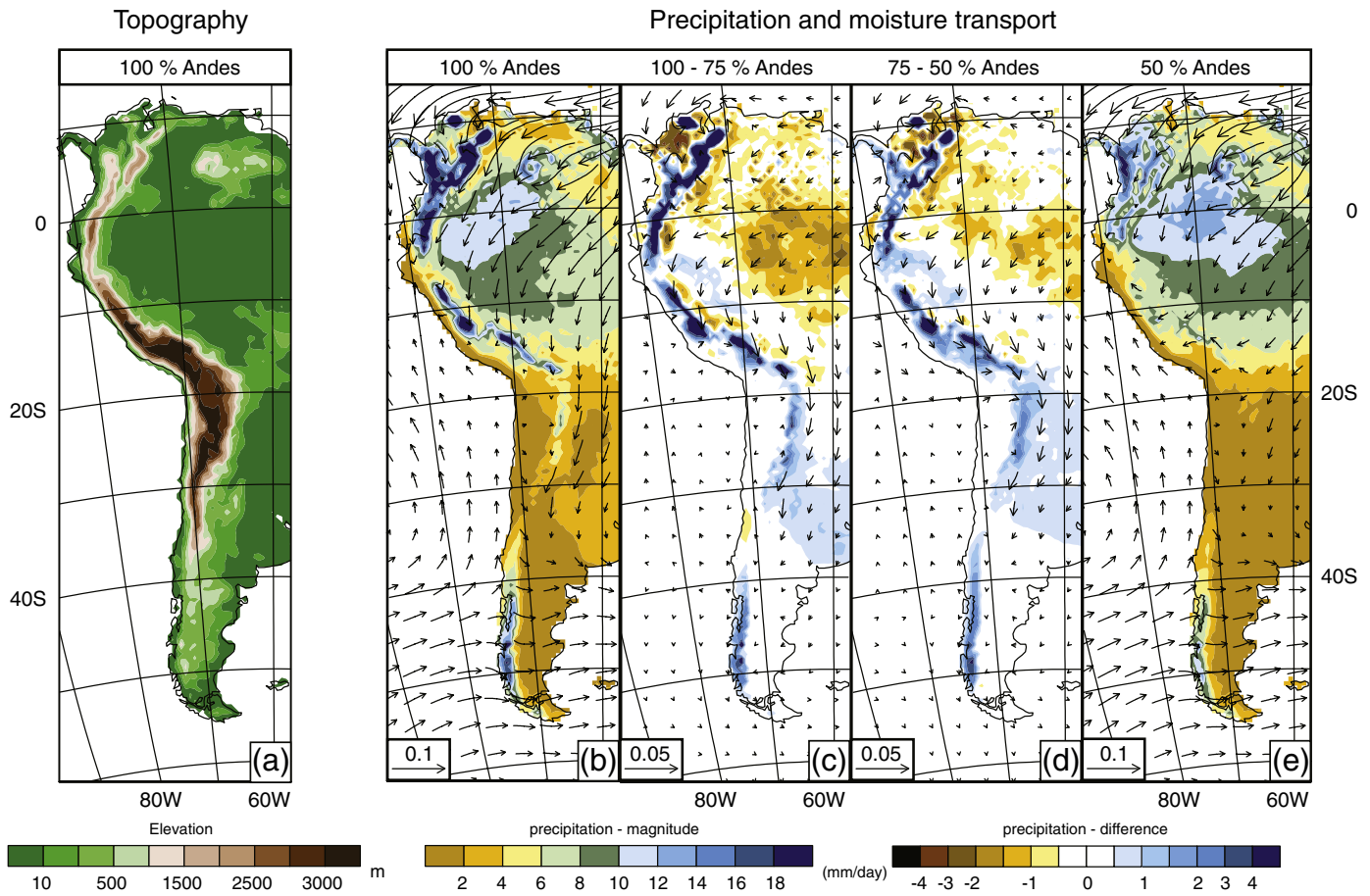### 100 % Andes

Precipitation and moisture transport

Fig. 3. Precipitation (mm/day) and low-level (850 mb) circulation over the Andes. (a) Present-day topography used in the model for 100% Andes simulations. (b–e) Changes in precipitation and low-level moisture transport (kg kg^{-1} m s^{-1}) between 50% and 100% Andean heights. (e) Absolute values of precipitation and moisture transport for 50% Andean height simulations, (d) difference in precipitation and moisture transport between 75 and 50% Andes, (c) difference in precipitation and moisture transport between 100 and 75% Andes, and (b) absolute precipitation and moisture transport values for simulations with 100% Andes, respectively.

with enhanced transport of isotopically enriched vapor from the South Pacific Ocean as a consequence of enhanced upward motion along the western flank. This upward motion is associated with intensified upper-level convergence over the Amazon Basin, which causes localized upper-level divergence over the western Andean flanks.

3.3. Sensitivity of isotopic lapse rates to surface uplift

The non-uniform $\delta^{18}O_p$ response to surface uplift over relatively small spatial scales impacts local isotopic lapse rates at different Andean heights. Due to interannual climate variability, annual oxygen isotopic lapse rates are variable and have large standard deviations from 10-year mean lapse rates (Fig. 2c–d, g–h). Nevertheless, we suggest that because proxy data represent conditions over thousands of years, interannual variations are averaged out and the means become significant. Changes in mean isotopic lapse rates reflect large-scale climatological changes associated with surface uplift and because changes in the isotopic ratios across and along the Andes are meaningful, changes in the mean $\Gamma_{\delta18O}$ represent actual changes in isotopic lapse rates in the past. Variability takes place on centennial and millennial timescales but changes on these timescales are beyond the scope of this paper.

When the Andes are lifted from 50 to 75% of modern elevation lapse rates along the eastern flank increase north of the AP (7–11°S) by up to > 0.5‰ km^{-1} (Fig. 2d) due to the simultaneous increase in $\delta^{18}O_p$ along the flank and decrease in $\delta^{18}O_p$ over the plateau region. Isotopic lapse rates decrease by ~0.7‰ km^{-1} across the southern AP (Fig. 2d), where $\delta^{18}O_p$ becomes more depleted at high and low

elevations. Along the western flank, isotopic lapse rates decrease with increasing elevation (Fig. 2h).

When the Andes are uplifted from 75 to 100% of modern elevations lapse rates along the eastern flank increase over the northern/central AP (up to 0.8‰ km^{-1}, Fig. 2c). The significant change in isotopic lapse rates is related to the strong decrease in $\delta^{18}O_p$ over most parts of the AP and simultaneous increase in $\delta^{18}O_p$ along the eastern Andean flank. North of this region (7–11°S), lapse rates slightly decrease (by 0.1–0.3‰ km^{-1}, Fig. 2c) due to an increase in $\delta^{18}O_p$ over the plateau region. Along the western flank, isotopic lapse rates significantly decrease north of the AP by almost 1‰ km^{-1} (Fig. 2g), most likely due to a reduction in the westward transport of continental air masses over the Andes (Fig. 3b). The Andes effectively block the moisture from the east, hindering transport of relatively light $\delta^{18}O_p$ from the continent.

4. Discussion

4.1. Effects of $\delta^{18}O$ and lapse rate changes on paleoaltimetry estimations

Our results demonstrate that $\delta^{18}O_p$ and isotopic lapse rates change substantially in response to regional climate change associated with Andean surface uplift. These findings are consistent with results from a lower resolution atmospheric global general circulation model that predicts non-uniform changes in $\delta^{18}O_p$ for Andean surface uplift from 0 to 50% and 50 to 100% of modern elevations, respectively (Poulsen et al., 2010). Our results indicate the existence of an elevation threshold that leads to dramatic changes in the $\delta^{18}O_p$ along the
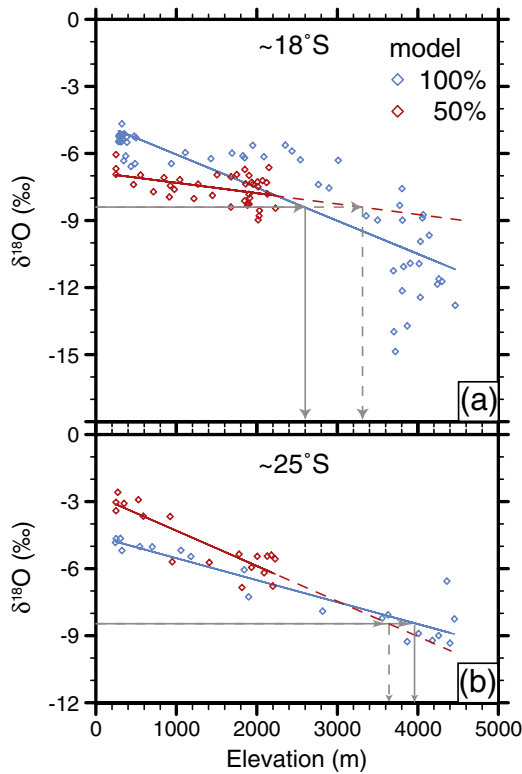
Fig. 4. Examples of $\delta^{18}O_p$–altitude relationships for model simulations with 100% and 50% Andean elevations across the Andean Plateau. Gray lines highlight the uncertainties in estimating paleoelevations from modern lapse rates. (a) $\delta^{18}O_p$–altitude relationship at approximately 18°S indicates larger modern lapse rates than 50% elevation lapse rates. Using a modern lapse rate to infer paleoelevations results in an underestimation of altitude. (b) Examples for $\delta^{18}O_p$–altitude relationship at approximately 25°S with modern lapse rates smaller than 50% elevation lapse rates. Using a modern lapse rate to infer paleoelevations results in an overestimation of altitude.

Andes due to the strengthening of the SALLJ and associated increase in rainout and Rayleigh distillation near 75% of modern Andean heights (~3000 m). The ≥5‰ depletion in $\delta^{18}O_p$ across the northern/central AP associated with the amount effect noticeably exceeds the ~1.5 to 2‰ $\delta^{18}O_p$ change expected from the modern altitude effect. North of the AP, the $\delta^{18}O_p$ increases by ~1.5‰ in response to surface uplift and associated changes in lower- and upper-level atmospheric circulation, a change that is opposite in sign than the altitude effect. These results demonstrate the sensitivity of stable isotopic compositions of meteoric water to factors other than elevation change and highlight the large uncertainties associated with paleoelevation reconstructions solely based on shifts in the $\delta^{18}O$ paleorecord.

Because the $\delta^{18}O_p$ response to surface uplift varies across the Andes, isotopic lapse rates also vary spatially with Andean elevation gain. Fig. 4 shows the $\delta^{18}O_p$–altitude relationship for the 100% and 50% Andean elevation simulations at ~18°S and 25°S, respectively, and indicates the uncertainty in estimating paleoelevations. For example, in the northern AP (Fig. 4a) using the modern oxygen isotopic lapse rate, a $\delta^{18}O_p$ composition of −8.5‰ would be interpreted to reflect an elevation of ~2600 m, while using an oxygen isotopic lapse rate calculated for the 50% scenario would lead to an altitude of ~3400 m. In contrast, in the southern AP a $\delta^{18}O$ change of −8.5‰ would be interpreted to reflect an elevation of ~4000 m using the modern stable isotopic lapse rate, while the 50% lapse rate would suggest an elevation of ~3600 m. These examples highlight that using a modern lapse rate to estimate paleoelevations can lead to either an under- or overestimation of past elevations.

We note that the isotopic lapse rates for different Andean height simulations are very similar when calculated for elevations below 3000 m. Observed precipitation-weighted mean $\delta^{18}O_p$ in the central Andes decreases by 1.5 to 2‰ over a 1500 m elevation gain (Gonfiantini et al., 2001), which is consistent with the low-elevation isotopic lapse rates of −0.5 to −1‰ km^{-1} simulated in our model (Fig. 5, Suppl. 1). However, $\delta^{18}O_p$ changes much more dramatic (~3‰ km^{-1}) at elevations above 3000 m. This is a consequence of non-linear convective processes at higher elevations. Because the isotopic composition of meteoric water is substantially more sensitive at high elevations, we suggest that a large shift of 3–4‰ in the paleodata is more consistent with changes at high elevations.

4.2. Miocene carbonate $\delta^{18}O$ response to Andean surface uplift

In the central Andes, a 3–4‰ depletion of $\delta^{18}O$ in ancient carbonate nodules has been interpreted to reflect changes in Andean surface elevation of 2.5 ± 1 km since the late Miocene (Garzione et al., 2006). This interpretation is based on using a modern isotopic lapse rate of approximately −1.4 to −2.3‰ km^{-1} (Gonfiantini et al., 2001) and suggests that the oldest carbonate samples (11.5 to 10.3 Ma) indicate paleoelevations of less than 1500 m and the youngest samples (6.8 to 5.5 Ma) represent modern elevations of >3800 m. Our results lead to a different interpretation.
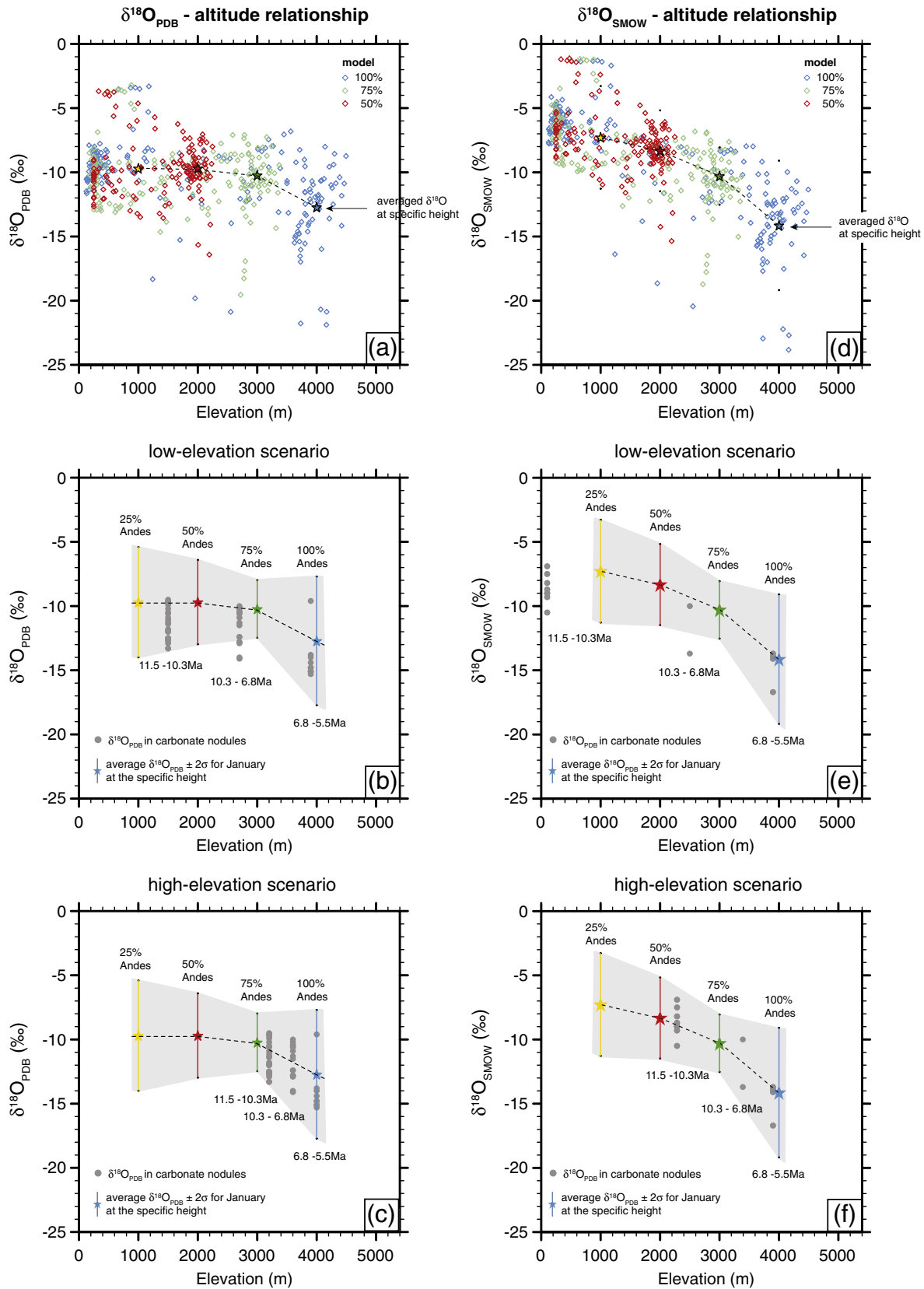
Fig. 5 shows the $\delta^{18}O$–altitude relationship for model simulations with 100%, 75%, and 50% Andean heights, and isotopic compositions derived from the ancient carbonate nodules that were sampled on the AP (Garzione et al., 2006). The fractionation of oxygen into the mineral calcite depends on the temperature during mineral formation. To directly compare proxy $\delta^{18}O_{PDB}$ from carbonates with simulated isotopic compositions, we calculate $\delta^{18}O_{PDB}$ based on simulated $\delta^{18}O_p$ in rainwater from which the carbonates grew, the simulated deep soil temperature (~8 m depth) at each point using our three elevation scenarios (50, 75, and 100%), and the equilibrium water-calcite oxygen isotopic fractionation factor (Kim and O'Neil, 1997). Due to a seasonal bias in pedogenic carbonate formation we only use the January model output for the calculation. Seasonality of carbonate formation is uncertain, but it has been suggested that in most settings carbonates mainly form during warm periods (Breecker et al., 2009; Quade et al., 2007). Thus, Andean carbonates most likely acquire their isotopic signature during the summer. Simulated January temperatures over the central Andes for different Andean heights are in the range of averaged carbonate growth temperatures based on clumped-isotope thermometry (see Section 4.3).

Fig. 5a shows the evolution of $\delta^{18}O_{PDB}$ across the central Andes with increasing surface elevation. Simulated averaged $\delta^{18}O_{PDB}$ is around −10‰ at elevations below 3000 m and decreases to around −12.5‰ at elevations above 3000 m (Fig. 5a). The isotopic response to elevation change over the Andean Plateau is not linear, but decreases substantially above ~75% Andean elevations. Previous studies have suggested that the $\delta^{18}O$ compositions in Miocene Andean carbonate nodules are consistent with a low elevation scenario (Fig. 5b). However, we note that the measured $\delta^{18}O_{PDB}$ are between −9.5 and −13.3‰ in older carbonates and between −13.8 and −15.3‰ in the younger carbonates (Garzione et al., 2006). Although these compositions mostly fall within the 2σ uncertainties of our model results, they represent substantially lower values than the average model $\delta^{18}O_{PDB}$ at the interpreted elevations. In addition, modern isotopic compositions of less than −10‰ in the central Andes are generally recorded at stations above 3000 m (Gonfiantini et al., 2001). Thus, we suggest that the $\delta^{18}O_{PDB}$ compositions of Miocene carbonate nodules are more consistent with a high-elevation scenario (Fig. 5c). The isotopic compositions of the ancient carbonate nodules are in good agreement with average $\delta^{18}O_{PDB}$ values at high elevations (Fig. 5c). Thus, they could be interpreted to represent paleoelevations

between 3000 and 4000 m and do not need to reflect fast and recent surface uplift. This interpretation is consistent with our model prediction that $\delta^{18}O_p$ decreases by over 5‰ when the Andes are uplifted from 75% to 100% modern heights (Fig. 1b).

4.3. Miocene Δ_{47}-clumped isotope response to Andean surface uplift

The hypothesis of fast and recent AP uplift is also based on reconstructed temperature changes and inferred paleoelevation

$\delta^{18}O_{PDB}$ - altitude relationship

(a)

$\delta^{18}O_{SMOW}$ - altitude relationship

(d)

low-elevation scenario

(b)

low-elevation scenario

(e)

high-elevation scenario

(c)

high-elevation scenario

(f)

reconstructions from paleobotany (Gregory-Wodzicki, 2000) and mass-47 isotopolog (Δ_{47}) compositions (Eiler et al., 2006; Ghosh et al., 2006a). In paleoaltimetry, clumped-isotope thermometry is used to estimate carbonate growth temperatures independently of the $\delta^{18}O$ of waters from which they formed (Ghosh et al., 2006b) and to compare estimated growth temperature to a known altitudinal gradient in surface temperature. On the AP, late Miocene carbonates show a temperature decline of 15.8 °C that has been interpreted to reflect 3400 ± 600 m of Andean surface uplift between 10.3 and 6.7 Ma based on the modern adiabatic lapse rate for the tropics of ~5 °C km^{-1} (Gonfiantini et al., 2001). However, the interpretation of Δ_{47} and inferred soil paleotemperatures are still a matter of debate (Eiler et al., 2006; Sempere et al., 2006). For example, Δ_{47}-estimated AP temperatures for the youngest carbonate samples (interpreted to reflect near-modern elevations) vary by ~14 °C over small spatial scales, a temperature range that is almost as large as the temperature difference between middle and late Miocene samples that has been interpreted to reflect >3000 m surface uplift (Ghosh et al., 2006b).

However, clumped-isotope derived paleotemperatures have been used to calculate $\delta^{18}O_{SMOW}$ values from late Miocene Andean carbonate samples (Ghosh et al., 2006b). Fig. 5d–f shows the $\delta^{18}O_{SMOW}$–altitude relationship for model simulations with 100, 75, and 50% Andean elevations and previously reported $\delta^{18}O_{SMOW}$. Fig. 5d indicates the non-linear response of $\delta^{18}O_{SMOW}$ with a threshold elevation at ~75% Andean heights and absolute $\delta^{18}O_{SMOW}$ values higher than -10‰ at elevations below 3000 m and ~-14‰ at higher elevations. Previously interpreted paleoelevations are systematically lower than what would be expected from the simulated $\delta^{18}O_p$–altitude relationship (Fig. 5e). We suggest that the isotopic compositions point to elevations above 50% of the modern Andes (Fig. 5f).

4.4. Caveats from modern boundary conditions

The objective of this study is to understand how uplift of the Andes influences meteoric $\delta^{18}O$ over the Andean Plateau region and to understand whether changes in isotopic compositions are mainly reflective of surface uplift itself or associated changes in regional climate. Our modeling results clearly demonstrate that topography has a non-linear and threshold effect on the isotopic composition of precipitation. We note that global changes during the Cenozoic (i.e. in large-scale ocean circulation and SST, the decline of atmospheric pCO_2, and evolution of land-surface), which are not accounted for in our simulations, complicate the comparison of simulated and observed $\delta^{18}O$ values.

The influences of changes in temperature (atmospheric CO_2 levels) and glaciations, as well as the presence of the South American inland seaway on Andean $\delta^{18}O_p$ have recently been quantified (Jeffery et al., 2011). According to these studies, $\delta^{18}O_p$ would likely have been ~2–3‰ higher as a result of warmer temperatures related to higher atmospheric CO_2 (3–4‰ increase in $\delta^{18}O_p$) and smaller ice volumes (~1‰ decrease in $\delta^{18}O_p$) (Jeffery et al., 2011; Poulsen and Jeffery, 2011). An inland seaway has the potential to lower $\delta^{18}O$ compositions over the Andean Plateau by 0–3‰, but uncertainty in the timing, geographic extent and isotopic composition of the South American inland seaway limits the ability to predict the absolute impact (Jeffery et al., 2011). In addition, several studies (Barreiro et al., 2006; Garreaud et al., 2010; Sepulchre et al., 2009) have suggested

that large-scale changes in the mean state of the Pacific (i.e. permanent El Niño conditions) lead to enhanced rainout along the central Andean coast. A permanent El Niño could cause a more northward position of the Bolivian High in comparison to its modern climatological mean position, which enhances westerly winds over the Andean Plateau and would result in higher $\delta^{18}O_p$ compositions in the past.

Moreover, it has been suggested that past changes in the distribution of the Amazon rainforest may have influenced the Amazon hydrological cycle (e.g. Cook and Vizy, 2008) and the $\delta^{18}O_p$ compositions of advected moisture. However, geological evidence (e.g. pollen histories, lake sediments, shells) suggests that the rainforest has existed in the Amazon Basin throughout the Cenozoic (e.g. Colinvaux and Oliveira, 2001; Hoorn, 2006; van der Hammen and Hooghiemstra, 2000).

Overall, the most substantial changes in $\delta^{18}O_p$ over the Andean Plateau related to changes in global boundary conditions are likely related to changes in global temperature and sea-surface temperatures. Both of these factors would drive simulated $\delta^{18}O_p$ compositions to higher values and therefore increase the discrepancy between observed and simulated $\delta^{18}O$ during the Miocene. Thus, we suggest that $\delta^{18}O_p$ compositions substantially lower than -10‰ generally reflect high (>3000 m) Andean surface elevations.

5. Implications

The work presented here focuses on the controversy about the timing and rate of Andean Plateau uplift and its influence on regional climate and $\delta^{18}O$. Fig. 6 shows a compilation of paleoelevation estimations mainly based on previous work listed in Barnes and Ehlers (2009) and more recent studies. Paleobotany work by Berry (1939) and Singewald and Berry (1922) suggest paleoelevations between 2000 and 2800 m, but they should be regarded with caution since errors are very large (± 2000 m). However, other paleobotany studies from Bolivia implying climate conditions consistent with a low-elevation (1160 ± 600 m m) AP in the middle to late Miocene (Graham et al., 2001; Gregory-Wodzicki et al., 1998; Muñoz and Charrier, 1996) are strongly debated. This discrepancy exists because the current leaf morphology methods systematically underestimate high altitudes (Kowalski, 2002) and it has been shown that the estimation of mean annual temperature at low-temperature (= high elevation) sites in Bolivia has an error ranging between 6.7 and 12.4 °C with an average of 9.3 °C (Kowalski, 2002). With a temperature lapse rate of ~5 °C km^{-1} (e.g. Gonfiantini et al., 2001) the more recent low late Miocene paleoelevations in the AP may be underestimated by 1.5–2.5 km. Consistent with this idea, a new study by Picard et al. (2008) estimates a paleoelevation of the southernmost Peruvian Andes of 2.0–2.5 km in the early Miocene (Fig. 6).

Paleoclimate reconstructions based on changes in soil compositions and mineral alterations (e.g., Alpers and Brimhall, 1988; Rech et al., 2006) have shown a significant shift towards more arid conditions along the western flank of the central Andes in the middle Miocene. The onset of hyperaridity during the middle Miocene in the Atacama Desert has been related to surface uplift and the creation of a rain shadow along the western flanks of the Andes, which leads to estimated minimum Andean paleoelevations of >2 km prior to 12–15 Ma (Fig. 6) (e.g., Alpers and Brimhall, 1988; Rech et al.,

Fig. 5. $\delta^{18}O$–altitude relationship for the central Andean Plateau from model results (25, 50, 75, and 100% of modern Andean elevations) and Miocene carbonates. In all panels, diamonds show simulated 10-year mean January $\delta^{18}O$ in the central Andes from individual grid points; stars represent the averaged simulated $\delta^{18}O$ compositions and 2σ variation for specific elevations (± 100 m). The gray shading highlights the range of 2σ variation. Gray circles represent paleodata. (a–c) Comparison of simulated and paleo $\delta^{18}O_{PDB}$ (from Garzione et al., 2006). We calculate model-derived $\delta^{18}O_{PDB}$ for each elevation case using simulated meteoric water $\delta^{18}O_p$ that would be in equilibrium with carbonate growth, simulated deep soil temperatures, and the equilibrium water-calcite oxygen isotopic fractionation factor (Kim and O'Neil, 1997). (d–f) Comparison of simulated and paleo $\delta^{18}O_p = \delta^{18}O_{SMOW}$. Proxy values have been calculated from $\delta^{18}O_{PDB}$ in late Miocene carbonates using temperatures derived from clumped isotope thermometry (Ghosh et al., 2006b). Note the strong decrease of $\delta^{18}O_{PDB}$ and $\delta^{18}O_{SMOW}$ between 3000 and 4000 m. In the low-elevation scenario, proxy data are substantially lower than the average model $\delta^{18}O$ at the interpreted elevations with certain $\delta^{18}O$ compositions even lower than the 2σ uncertainty range. We propose a high-elevation scenario with paleo $\delta^{18}O$ values representing paleoelevations between 3000 and 4000 m.
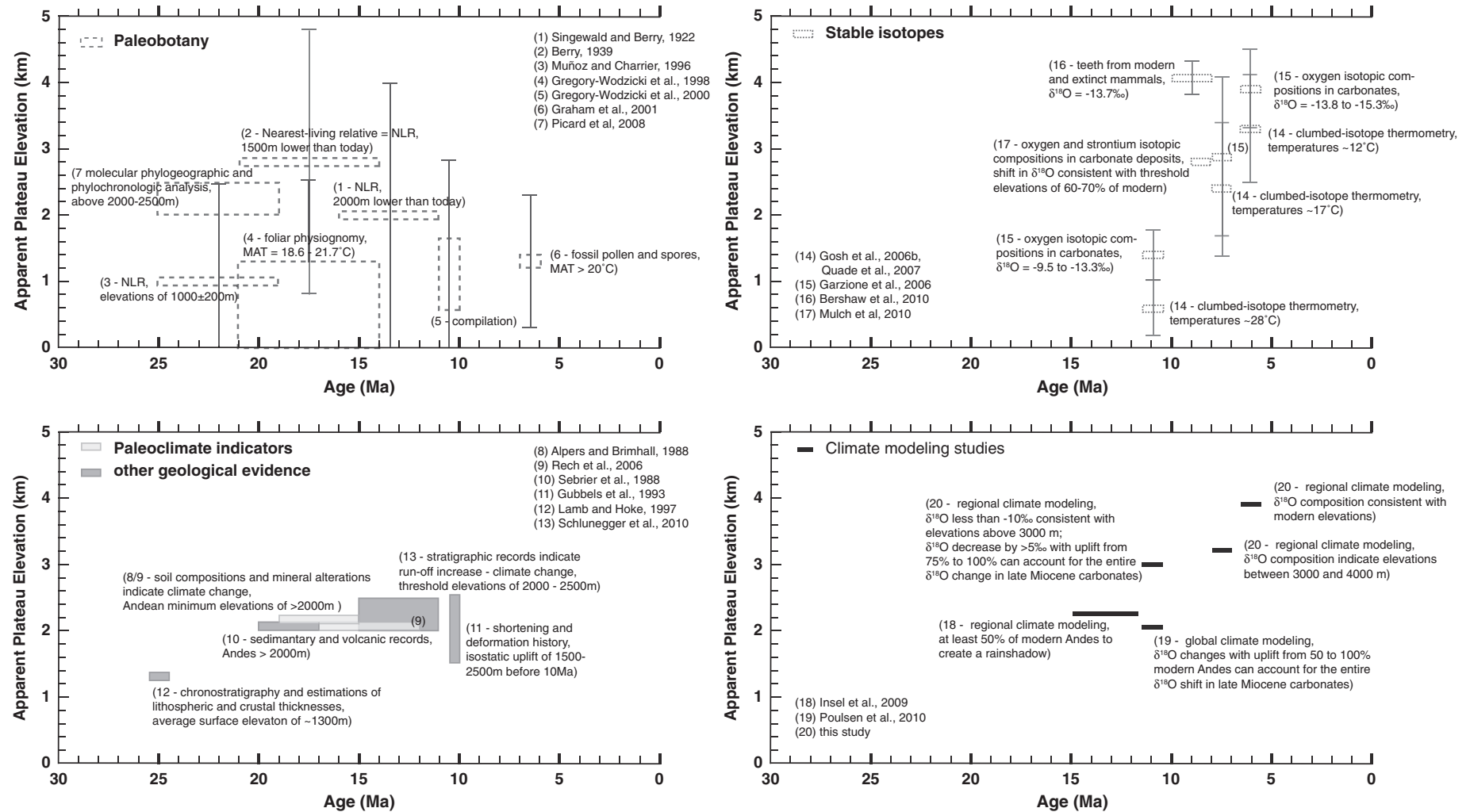
Fig. 6. Summary of paleoelevation estimates for the central Andes based on (a) paleobotany, (b) paleoclimate and geological evidence, (c) stable isotope analyses, and (d) climate modeling studies. Apparent plateau elevation (km) is plotted against age (Ma). Gray boxes represent the elevation and age range of estimates from previous studies. The black lines from the climate modeling studies indicate minimum elevations. Paleobotany and stable isotope studies have been mostly interpreted to reflect low elevations before 10 Ma. Paleoclimate indicators, sedimentological and structural data, and climate modeling studies indicate substantial Andean heights between 20 and 10 Ma. Note that the low-elevation stable isotope data would plot at substantially higher elevations if interpreted to not only reflect surface uplift, but also regional climate change.

2006). Consistent with this conclusion, results from global and regional general circulation models indicate that at least half the modern Andean elevation is necessary to block westerly flow and establish easterlies that bring moisture from the Amazon Basin to the eastern Andean flank and establish arid conditions along the western Andean side (Fig. 6) (Ehlers and Poulsen, 2009, Insel et al., 2009). Other geological evidence based on sedimentological, structural, and volcanic records suggest that the Andes had already risen considerably and could not have been less than 2000–2500 m high in the Middle Miocene (Fig. 6) (e.g., Gubbels et al., 1993; Schlunegger et al., 2010; Sebrier et al., 1988) and ~1300 m by late Oligocene times (Lamb and Hoke, 1997)

In addition, new stable isotope data from late Miocene fossil teeth that are similar to modern suggest that by ~8 Ma the northern Altiplano had reached high elevation and established a latitudinal rainfall gradient similar to modern (Fig. 6) (Bershaw et al., 2010). A rapid shift in $\delta^{18}O$ of pedogenic carbonates in the Chaco foreland basin at ~8 Ma has been ascribed to the attainment of threshold elevations of the central Andes that are necessary to significantly modulate South American precipitation patterns and are therefore consistent with Andean elevations of 60–70% of its modern elevation around that time (Mulch et al., 2010).

Our results in combination with other geological and climatological evidence suggest that the Andean Plateau did not experience a 2.5 km rapid and recent rise in the late Miocene. Numerous studies indicate that the central Andes likely have been at 2000–2500 km between 25 and 11 Ma (Fig. 7) (e.g. Alpers and Brimhall, 1988; Insel et al., 2009; Picard et al., 2008; Rech et al., 2006; Schlunegger et al., 2010; Sebrier et al., 1988; Singewald and Berry, 1922). Paleobotany data are consistent with this interpretation, assuming that previously interpreted low Andean elevations (Gregory-Wodzicki et al., 1998; Gregory-Wodzicki, 2000; Muñoz and Charrier, 1996) underestimate true paleoelevations by 1.5–2.5 km (Kowalski, 2002). Between 11 and 6 Ma changes in carbonate $\delta^{18}O$ and Δ_{47} have been used to infer rapid Andean surface uplift (Garzione et al., 2006; Ghosh et al., 2006b). However, our results in agreement with previous climate modeling studies (e.g. Poulsen et al., 2010) indicate that significant modifications in moisture sources, transport, and availability occur when the Andes attain a threshold elevation of 2.5 to 3 km. Fig. 5a and d shows an abrupt decrease in $\delta^{18}O_p$ that is not necessarily related to an increase in surface uplift rate, but rather indicates the attainment of a threshold elevation that causes climatic changes which influence amount and source effects. Our results show that $\delta^{18}O$ is influenced by processes not accounted for in traditional paleoaltimetry estimates and that paleoclimate modeling studies are necessary to provide additional constrains on the interpretation of soil carbonate $\delta^{18}O$ records and to redefine the uplift history of the Andes. Based on all the data, Andean uplift may have been slow and steady since before Neogene times or stepwise with minor uplift pulses including one between 10 and 6 Ma (Fig. 7), but the data do not support a large rapid uplift event in the Late Miocene.

6. Conclusions

In conclusion, we find that the Late Miocene change in $\delta^{18}O_p$ is most likely due to a combination of surface uplift and associated regional climate change. We suggest that the 3–4‰ change in $\delta^{18}O$ in ancient carbonate nodules reflects an increase in precipitation and Rayleigh distillation during Andean surface uplifted from 75 to 100% of modern elevations. The reasons for our conclusion are:

(1) Model simulations and modern isotope data from climatological stations suggest that isotopic compositions lower than −10‰ generally reflect fractionation processes at elevations above 3000 m. The $\delta^{18}O$ composition of the ancient carbonate nodules is generally smaller than −10‰ suggesting a paleoelevation of above 3000 m.

(2) Model results indicate that $\delta^{18}O_p$ decreases by >5‰ with AP surface uplift from 75% to 100% of modern elevations due to changes in the low-level (850 mb) atmospheric circulation and precipitation. This isotopic depletion accounts for the entire change in the isotopic composition of carbonate nodules between 10 and 6 Ma. This result is consistent with the assumption that the soil $\delta^{18}O$ represents a paleoelevation of above 3000 m (which is equivalent to 75% Andes).

(3) Carbonate growth temperatures derived from clumped-isotope thermometry show a large variability that is not completely understood and may reflect processes other than adiabatic cooling. In addition, when using these temperatures to estimate $\delta^{18}O_{SMOW}$ values, the calculated isotopic compositions are inconsistent with observed $\delta^{18}O_p$ at low elevations, but are consistent with our new interpretation of late Miocene Andean elevations of >3000 m.

(4) Isotopic lapse rates have large interannual variability. Short-term observations of modern isotopic lapse rates may not represent mean climatic conditions. As a result, paleoelevation
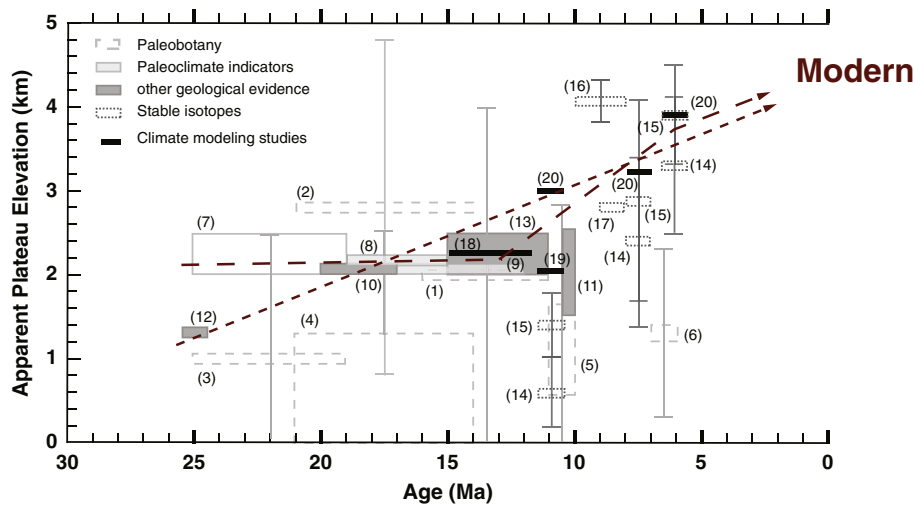

Fig. 7. Re-evaluated paleoelevation history of the central Andes. Gray boxes and numbers refer to previous studies from Fig. 6. Red arrows show possible surface uplift histories of the central Andes since 25 Ma. Compilation of all data suggests slow and steady uplift since the early Miocene or a stepwise uplift scenario with minor surface uplift between 10 and 6 Ma.

interpretations based on these lapse rates may include large errors. Moreover, we demonstrate that isotopic lapse rates change with surface uplift and can lead to substantial misinterpretations of paleoelevations.

Supplementary materials related to this article can be found online at doi:10.1016/j.epsl.2011.11.039.

Acknowledgment

References

Alpers, C.N., Brimhall, G.H., 1988. Middle Miocene climate change in the Atacama Desert, northern Chile: evidence from supergene mineralization at La Escondida. Geol. Soc. Am. Bull. 100, 1640–1656.

Barnes, J.B., Ehlers, T., 2009. End member models for Andean Plateau uplift. Earth Sci. Rev. 97 (1–4), 105–132.

Barreiro, M., Philander, G., Pacanowski, R.C., Fedorov, A.V., 2006. Simulations of warm tropical conditions with application to middle Pliocene atmospheres. Clim. Dyn. 26, 349–365.

Berry, E.W., 1939. The fossil flora of Potosi, Bolivia. Johns Hopkins University Studies in Geology 13, 1–67.

Bershaw, J., Garzione, C.N., Higgins, P., MacFadden, B.J., Anaya, F., Alvarenga, H., 2010. Spatial–temporal changes in Andean plateau climate and elevation from stable isotopes of mammal teeth. Earth Planet. Sci. Lett. 289, 530–538.

Breecker, D.O., Sharp, Z.D., MacFadden, L.D., 2009. Seasonal bias in the formation and stable isotopic composition of pedogenic carbonate in modern soils from central New Mexico, USA. GSA Bull. 121 (3–4), 630–640.

Chamberlain, C.P., Poage, M., Craw, D., Reynolds, J., 1999. Topographic development of the Southern Alps recorded by the isotopic composition of authigenic clay minerals, South Island, New Zealand. Chem. Geol. 155, 279–294.

Colinvaux, P.A., Oliveira, P.E., 2001. Amazon plant diversity and climate through the Cenozoic. Palaeogeogr. Palaeoclimatol. Palaeoecol. 166, 51–63.

Cook, K.H., Vizy, E.K., 2008. Effects of twenty-first-century climate change on the Amazon Rain Forest. J. Clim. 21, 542–560.

Drummond, C.N., Wilkinson, B.H., Lohmann, K.C., Smith, G.R., 1993. Effect of regional topography and hydrology on the lacustrine isotopic record of Miocene paleoclimate in the Rocky Mountains. Palaeogeogr. Palaeoclimatol. Palaeoecol. 101, 67–79.

Ehlers, T., Poulsen, C.J., 2009. Influence of Andean uplift on climate and paleoaltimetry estimates. Earth Planet. Sci. Lett. 281, 238–248.

Eiler, J., Garzione, C.N., Ghosh, P., 2006. Response to Comments on "Rapid uplift of the Altiplano revealed through ^{13}C–^{18}O bonds in paleosol carbonates". Science 314, 760c.

Garreaud, R., Molina, A., Farias, M., 2010. Andean uplift, ocean cooling and Atacama hyperaridity: a climate modeling perspective. Earth Planet. Sci. Lett. 292, 39–50.

Garzione, C.N., Hoke, G., Libarkin, J.C., Withers, S., MacFadden, B., Eiler, J., Ghosh, P., Mulch, A., 2008. Rise of the Andes. Science 230 (1304). doi:10.1126/science.1148615.

Garzione, C.N., Molnar, P., Libarkin, J., MacFadden, B., 2006. Rapid late Miocene rise of the Bolivian Altiplano: evidence for removal of mantle lithosphere. Earth Planet. Sci. Lett. 241, 543–556.

Ghosh, P., Adkins, J., Affek, H., Balta, B., Guo, W., Schauble, E.A., Schrag, D., Eiler, J.M., 2006a. ^{13}C–^{18}O bonds in carbonate minerals: a new kind of paleothermometer. Geochim. Cosmochim. Acta 70, 1439–1456.

Ghosh, P., Garzione, C., Eiler, J., 2006b. Rapid uplift of the Altiplano revealed through ^{13}C–^{18}O bonds in paleosol carbonates. Science 311, 511–515.

Gonfiantini, R., Roche, M.-A., Olivry, J.-C., Fontes, J.-C., Zuppi, G.M., 2001. The altitude effect on the isotopic composition of tropical rains. Chem. Geol. 181, 147–167.

Graham, A., Gregory-Wodzicki, K.M., Wright, K.L., 2001. Studies in neotropical paleobotany. XV. A Mio-Pliocene Palynoflora from the Eastern Cordillera, Bolivia: implications for the uplift history of the central Andes. Am. J. Bot. 88 (9), 1545–1557.

Gregory-Wodzicki, K., McIntosh, W., Velasquez, K., 1998. Climatic and tectonic implications of the late Miocene Jakokkota Flora, Bolivian Altiplano. J. S. Am. Earth Sci. 11 (6), 533–560.

Gregory-Wodzicki, K.M., 2000. Uplift history of the Central and Northern Andes; a review. Geol. Soc. Am. Bull. 112 (7), 1091–1105.

Gubbels, T.L., Isacks, B.L., Farrar, E., 1993. High-level surfaces, plateau uplift, and foreland development, Bolivian Central Andes. Geology 21 (8), 695–698.

Hoffmann, G., Werner, M., Heimann, M., 1998. Water isotope module of the ECHAM atmospheric general circulation model: a study on timescales from days to several years. J. Geophys. Res. 103 (D14), 16871–16896.

Hoorn, C., 2006. The birth of a mighty Amazon. Sci. Am. 294 (5), 52–59.

Insel, N., Poulsen, C.J., Ehlers, T.A., 2010. Influence of the Andes mountains on South American moisture transport, convection, and precipitation. Clim. Dyn. 35, 1477–1492. doi:10.1007/s00382-00009-00637-00381.

Jeffery, M. L., Poulsen, C. J., and Ehlers, T. A., 2011, Impacts of Cenozoic global cooling, surface uplift and an inland seaway on South American paleoclimate and precipitation d18O: AGU, GSA Bulletin, doi:10.1130/B30480.1.

Kim, S.-T., O'Neil, J.R., 1997. Equilibrium and nonequilibrium oxygen isotope effects in synthetic carbonates. Geochim. Cosmochim. Acta 61 (16), 3461–3475.

Kowalski, E.A., 2002. Mean annual temperature estimation based on leaf morphology: a test from tropical South America: palaeogeography. Palaeogeogr. Palaeoclimatol. Palaeoecol. 188, 141–165.

Lamb, S., Hoke, L., 1997. Origin of the plateau in the central Andes, Bolivia, South America. Tectonics 16 (4), 623–649.

Mulch, A., Uba, C., Strecker, M.R., Schoenberg, R., Chamberlain, C.P., 2010. Late Miocene climate variability and surface elevation in the central Andes. Earth Planet. Sci. Lett. 290, 173–182.

Muñoz, N., Charrier, R., 1996. Uplift of the western border of the Altiplano on a west-vergent thrust system, Northern Chile. J. S. Am. Earth Sci. 9 (3–4), 171–181.

Picard, D., Sempere, T., Plantard, 2008. Direction and timing of uplift propagation in the Pervian Andes deduced from molecular phylogenetics of highland biotaxa. Earth Planet. Sci. Lett. 271, 326–336.

Poulsen, C.J., Ehlers, T., Insel, N., 2010. Onset of convective rainfall during gradual late Miocene rise of the central Andes. Science 328, 490–493. doi:10.1126/science.1185078.

Poulsen, C.J., Jeffery, M.L., 2011. Climate change imprinting on stable isotopic compositions of high-elevation meteoric water cloaks past surface elevations of major orogens. Geology 39 (6), 595–598. doi:10.1130/G32052.32051.

Quade, J., Garzione, C., Eiler, J., 2007. Paleoelevation reconstructions using pedogenic carbonates. Rev. Mineral. Geochem. 66, 53–87.

Rech, J.A., Currie, B.S., Michalski, G., Cowan, A.M., 2006. Neogene climate change and uplift in the Atacama Desert, Chile. Geology 34 (9), 761–764.

Schlunegger, F., Kober, F., Zeilinger, G., von Rotz, R., 2010. Sedimentology-based reconstructions of paleoclimate changes in the Central Andes in response to the uplift of the Andes, Arica region between 19 and 21°S latitude, northern Chile. Int. J. Earth Sci 99, 123–137. doi:10.1007/s00531-00010-00572-00538.

Sebrier, M., Lavenu, A., Fornari, M., Soulas, J.P., Anonymous, 1988. Tectonics and uplift in Central Andes (Peru, Bolivia and northern Chile) from Eocene to present, Seminaire. Geodynamique des Andes centrales. Seminar on Geodynamics of the Central Andes, Volume 3: Bondy. Office de la Recherche Scientifique et Technique Outre-Mer (ORSTOM), pp. 85–106.

Sempere, T., Hartley, A.J., Roperch, P., 2006. Comment on "Rapid uplift of the Altiplano revealed through ^{13}C–^{18}O bonds in paleosol carbonates". Science 314, 760.

Sepulchre, P., Sloan, L.C., Snyder, M., Fiechter, J., 2009. Impacts of Andean uplift on the Humboldt Current system: a climate model sensitivity study. Paleoceanography 24 (PA4215). doi:10.1029/2008PA001668.

Siegenthaler, U., Oeschger, H., 1980. Correlation of ^{18}O in precipitation with temperature and altitude. Nature 285, 314–317.

Singewald, J.T., Berry, E.W., 1922. The geology of the Corocoro copper district of Bolivia. Johns Hopkins University Studies in Geology 1, 1–117.

Stern, L.A., Blisniuk, P.M., 2002. Stable isotope composition of precipitation across the southern Patagonian Andes. J. Geophys. Res. 107(D23 (4667). doi:10.1029/2002JD002509.

Sturm, C., Hoffmann, G., Langmann, B., 2007a. Simulation of the stable water isotopes in precipitation over South America: comparing regional to global circulation models. J. Clim. 20, 3730–3750.

Sturm, C., Vimeux, F., Krinner, G., 2007b. Intraseasonal variability in South America recorded in stable water isotopes. J. Geophys. Res. 112. doi:10.1029/2006JD008298.

Sturm, K., Hoffmann, G., Langmann, B., Stichler, W., 2005. Simulation of $\delta^{18}O$ in precipitation by the regional circulation model REMOiso. Hydrol. Process. 19, 3425–3444.

van der Hammen, T., Hooghiemstra, H., 2000. Neogene and Quaternary history of vegetation, climate, and plant diversity in Amazonia. Quat. Sci. Rev. 19, 725–742.

Vuille, M., Bradley, R.S., Werner, M., Healy, R., Keimig, F., 2003. Modeling $\delta^{18}O$ in precipitation over the tropical Americas: 1. Interannual variability and climatic controls. J. Geophys. Res. 108 (D6). doi:10.1029/2001JD002038.